Progress in Neurobiology 260 (2026) 102904

Contents lists available at ScienceDirect

Progress in Neurobiology

journal homepage: www.elsevier.com/locate/pneurobio

# The VGLUT3 positive neurons of the median raphe region promote long-term spatial memory through time-dependent mechanisms

Csilla Lea Fazekas [a,b,c,d,e], Bibiána Török [a,e], Adrienn Szabó [a,d,e], Pedro Correia [a,d,e], Tiago Chaves [a,d,e], Véronique Fabre [b,c], Stéphanie Daumas [b,c,*], Dóra Zelena [a,e,**,1]

[a] Laboratory of Behavioral and Stress Studies, Institute of Experimental Medicine, Szigony utca 43, Budapest 1083, Hungary
[b] Sorbonne Université, CNRS, Inserm, Centre of Neuroscience, NeuroSU, Paris F-75005, France
[c] Sorbonne Université, CNRS, Inserm, Institut de Biologie Paris-Seine, IBPS, Paris F-75005, France
[d] János Szentágothai School of Neurosciences, Semmelweis University, Üllői út 26, Budapest 1085, Hungary
[e] Institute of Physiology, Medical School, University of Pécs, Centre for Neuroscience, Szentágothai Research Centre, Szigeti út 12, Pécs 7624, Hungary

ARTICLE INFO

*Keywords:*
Learning
Memory
Median raphe
VGLUT3
Watermaze
Chemogenetics
Optogenetics

ABSTRACT

Episodic memory and related forms of learning depend critically on the hippocampus, whose activity is regulated by brainstem inputs that remain incompletely understood. The midbrain median raphe region (MRR) is a key regulator of forebrain circuits and, while classically recognised as serotonergic, many of its neurons also release glutamate. Notably, a subset of MRR neurons projecting to the hippocampus expresses the vesicular glutamate transporter type 3 (VGLUT3), suggesting a glutamatergic contribution. Moreover, electrophysiological data indicate that these MRR-VGLUT3 + neurons influence hippocampal oscillations and therefore, hippocampus-dependent learning and memory. Our goal was to investigate the role of MRR-VGLUT3 + neurons in hippocampus-dependent learning and memory. Using VGLUT3-Cre mice of both sexes, we employed adeno-associated viral vectors to selectively activate MRR-VGLUT3 + neurons during the water maze task, a known hippocampus-dependent behavioural paradigm. Neuronal excitation was achieved by chemogenetics (DREADDs) or, to probe temporally restricted effects, by optogenetics (Channelrhodopsin2) during the spatial reference memory phase. Given the involvement of MRR and VGLUT3 + neurons in locomotion and anxiety-like behaviours, open field and elevated plus maze assays were also performed but yield inconclusive results. We found that chronic chemogenetic excitation did not alter learning but enhanced long-term memory performance, a finding replicated in an independent cohort. In contrast, acute optogenetic excitation had no effect, suggesting that MRR-VGLUT3 + neurons may contribute to memory related processes in a temporally specific manner.

## 1. Introduction

Learning and memory are complex physiological process supported by interactions across multiple brain regions. Among these, the hippocampus is a central structure, essential for episodic (Danieli et al., 2023) and spatial memory (Vann and Albasser, 2011). In addition, to cortical inputs, brainstem structures also influence hippocampal function, though their regulatory mechanisms remain less well understood.

The median raphe region (MRR) is one of the midbrain raphe nuclei that provides serotonergic projections to the forebrain. It heavily innervates the hippocampus (Kohler and Steinbusch, 1982; Freund, 1992; McKenna and Vertes, 2001) and regulates hippocampal ripples and theta oscillations (Wang et al., 2015a; Bland et al., 2016), thereby potentially influencing learning and memory (Almada et al., 2009; Wang et al., 2015a; He et al., 2022). A key role of the MRR is hippocampal desynchronization (Maru et al., 1979; Jackson et al., 2008; Crooks et al., 2012), achieved in part through the excitation of local inhibitory interneurons (Freund et al., 1990; Varga et al., 2009). Despite this well-established physiological role, the behavioural effects of MRR activity on learning and memory are often controversial or context specific. For instance, optogenetic stimulation of the MRR after contextual fear memory training impaired memory consolidation (Wang

* Corresponding author at: Sorbonne Université, CNRS, Inserm, Centre of Neuroscience, NeuroSU, Paris F-75005, France.
** Corresponding author at: Laboratory of Behavioral and Stress Studies, Institute of Experimental Medicine, Szigony utca 43, Budapest 1083, Hungary.
*E-mail addresses:* stephanie.daumas@sorbonne-universite.fr (S. Daumas), zelena.dora@pte.hu (D. Zelena).
[1] Dóra Zelena will handle correspondance at all stages of the refereeing and publication process and also post-publication

https://doi.org/10.1016/j.pneurobio.2026.102904
Received 23 October 2025; Received in revised form 25 February 2026; Accepted 3 March 2026
Available online 7 March 2026

et al., 2015a), whereas our previous work demonstrated that optogenetic stimulation enhanced remote contextual fear memory, while inhibition impaired it (Balazsfi et al., 2017). The relevance of MRR function to memory processes is further supported by evidence linking the serotonergic system to Alzheimer's disease (AD), one of the most common dementias (Geldenhuys and Van der Schyf, 2011; Eremin et al., 2023). In animal studies, MRR lesions caused long-term memory (LTM) deficits (Melik et al., 2000; Silva et al., 2002), but spared acquisition or short-term memory (STM) in contextual fear paradigms (Melik et al., 2000).

Overall, these findings support a regulatory role of the MRR in learning and memory, which may be mediated via parallel serotonergic and non-serotonergic systems (Crooks et al., 2012). A substantial proportion of MRR neurons are glutamatergic, characterised by the expression of vesicular glutamate transporters (VGLUT) (Gras et al., 2002; Jackson et al., 2009; Sos et al., 2017; Szonyi et al., 2019). Among these, VGLUT3 (Fremeau et al., 2002; Schafer et al., 2002) is frequently co-expressed with other primary neurotransmitters (Gras et al., 2008; Zander et al., 2010). Within the MRR, a significant proportion of neurons are non-serotonergic-VGLUT3 + , alongside serotonergic-VGLUT3 + neurons (Sos et al., 2017). MRR-VGLUT3 + terminals densely innervate the hippocampus and, in the CA1 region, form functional NMDA receptor-containing synapses on local interneurons (Szonyi et al., 2016; Fortin-Houde et al., 2023). It has been proposed that non-serotonergic MRR neuronal populations coupled to hippocampal theta and ripple oscillations are glutamatergic (Viana Di Prisco et al., 2002; Wang et al., 2015a). Consistently, the inhibitory influence of MRR on hippocampal ripple events proved to be only partially serotonergic (and indirectly GABAergic), suggesting that glutamatergic neurons mediate the profound inhibition of ripple activity (Wang et al., 2015a). Supporting this, serotonergic MRR neurons exhibit little coupling to hippocampal theta oscillations, whereas VGLUT3 + neurons show strong coupling (Huang et al., 2022). Together, these anatomical and electrophysiological findings point to a critical role of the MRR glutamatergic neurons in regulating hippocampal network activity. However, their specific contribution to hippocampus-dependent behaviours remains unknown.

We aimed to investigate how MRR-VGLUT3 + neuronal activity influences hippocampus-dependent learning and memory in the Watermaze (WM) behavioural paradigm. Because both MRR and VGLUT3 + neurons have been implicated in locomotion and anxiety-like behaviours (Amilhon et al., 2010; Bland et al., 2016; Abela et al., 2020; Kljakic et al., 2022), animals were also screened in the open field (OF) and elevated plus maze (EPM) tests to control for possible confounding factors. To achieve cell-specific excitation, we used VGLUT3-Cre mice and Cre-dependent viral vectors encoding either excitatory designer receptors (chemogenetics) or Channelrhodopsin2 (optogenetics).

Reproducibility was explicitly addressed through an independent replication cohort of chemogenetic experiments conducted in another lab, thereby strengthening the reliability of our findings (Munafo et al., 2017). Concerns have been raised about behavioural variability in neuroscience research, particularly due to extensive inbreeding of mouse strains, which can produce divergent phenotypes not only across strains but potentially across laboratories, sometimes yielding contradictory results (Montkowski et al., 1997; Van Dam et al., 2006; Matsuo et al., 2010; Sultana et al., 2019). This issue has been highlighted as part of the so-called reproducibility crisis in science (Munafo et al., 2017). To address this, chemogenetic experiments were conducted in two differently bred VGLUT3-Cre mouse lines (one locally engineered and one commercially acquired) across two independent laboratories located in France and Hungary. Chemogenetics was performed at Sorbonne Université (Paris, France), while both chemogenetics and optogenetics were conducted at the Institute of Experimental Medicine (Budapest, Hungary). Experimental protocols, handling procedures, and environmental conditions were standardized across sites unless otherwise specified.

## 2. Materials and methods

### 2.1. Animals

All VGLUT3-Cre male and female mice were obtained from local colonies. In France, animals on a C57BL/6 N background were bred locally from heterozygous breeding pairs and genotyped by PCR, while in Hungary, the colony was established from an original breeding pair obtained from Jackson Laboratories (strain # 018147), originating from homozygous breeding pairs. Mice were housed in groups of 2–5 in Macrolon cages (40 × 25 × 26 cm) under a standard 12-hour light–dark cycle (lights on at 7 a.m., 21 ± 1°C, 50–60% humidity), with food (standard mice chow, Charles River) and tap-water available *ad libitum*. All animals were accustomed to handling for 3–4 days before the start of the experiments.

All animal procedures were approved by the relevant animal care committees: Sorbonne Université (Ministère de l'Agriculture et de la Forêt, Service Vétérinaire de la Santé et de la Protection Animale, authorization #01482.01, ethics committee Darwin #5) and the Institute of Experimental Medicine (Workplace Animal Welfare Committee of Institute of Experimental Medicine and National Scientific Ethical Committee on Animal Experimentation of Hungary; PEI/001/33–4/2013, PE/EA/254–7/2019). Experiments were conducted in accordance with the European Communities Council Directive recommendations for the care and use of laboratory animals (2010/63/EU). The study complied with the ARRIVE guidelines.

### 2.2. Surgery

VGLUT3-Cre mice underwent stereotaxic surgery (David Kopf Instruments) as described previously (Balazsfi et al., 2017, 2018; Fazekas et al., 2021; Chaves et al., 2022). Surgeries were performed under anaesthesia with a mixture of ketamine (100 mg/kg) and xylazine (10 mg/kg). Cre-dependent adeno-associated viral vectors (AAVs from Addgene, details bellow) were injected into the MRR (AP: −4.1 mm; L: 0 mm; DV: 4.6 mm from Bregma) (Fig. 1**a**).

For chemogenetic experiments (France: main dataset; Hungary: extended dataset), the injected AAV (serotype 8, 40 nL) encoded either excitatory designer receptors exclusively activated by designer drugs (DREADDs) with red fluorescent protein (RFP) as reporter (Addgene #44361; n = 6♀6♂) or RFP only (Addgene #50459; n = 6♀7♂). Animals were allowed 14 days recovery and viral expression period before behavioural testing. The replication study conducted in Hungary strictly followed the same procedures. Additional details and necessary differences are provided in Supplementary Data. In a preliminary experiment an additional group was included, which expressed inhibitory DREADDs (Addgene #44362; n = 4♀3♂) and RFP. However, due to experimental animal availability and lack of effect on the behavioural outcome in the WM task, this group was omitted from further experimental designs. The preliminary results of this experiment can be seen in Supplementary Figure 2, which shows the results from Fig. 2**a-d** for the control and excitatory groups, alongside the inhibitory group (black). The statistical tests do not contain the dataset of the inhibitory group.

For optogenetic experiments (Hungary), AAVs (serotype 5, 40 nL, Addgene #26973) encoded Channelrhodopsin2 (ChR2) with enhanced yellow fluorescent protein (EYFP) as a reporter protein in the excitatory group (n = 6♀7♂) (Balazsfi et al., 2017, 2018). Control animals (Addgene #27056, n = 4♀8♂) received viral injections encoding only EYFP. Two weeks post-surgery, custom-made optic fibres (multimode optical fibres, flat tip, 0.22 NA, low-OH Ø105 μm core, FG105LCA, Thorlabs Corp.; flanged zirconia ferrule [LC MM C35 Chamfer Ferrule 127 μm with Flange, Senko]) were implanted above the MRR (AP: −4.8 mm; L:0 mm; DV: −4.1 mm; 10° inclination to posterior) and secured to the skull with screws and acrylic resin (Duracryl Plus; SpofaDental). Following surgery, animals were housed individually and allowed a further 2-week recovery period. During the last five days of

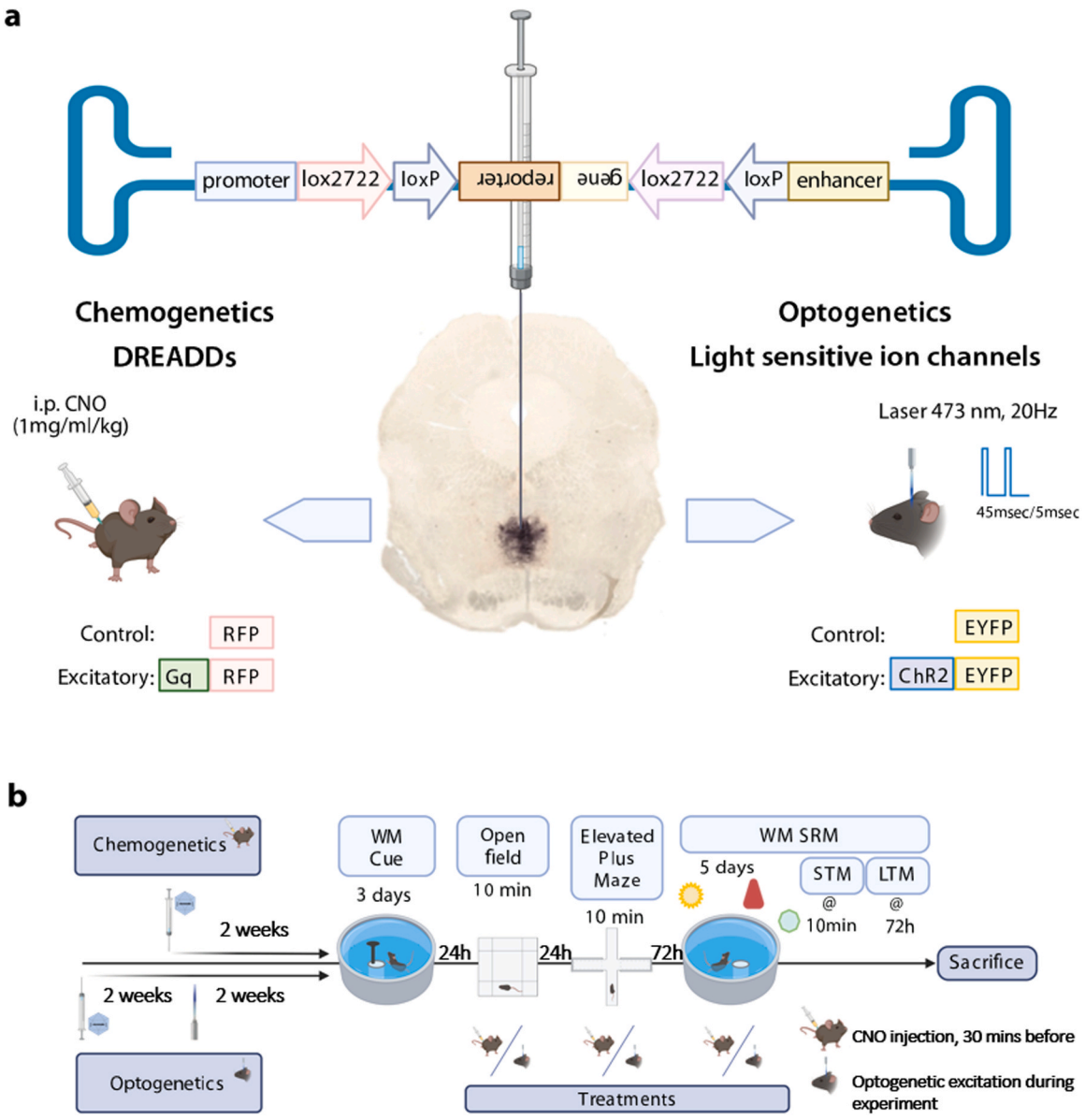


**Fig. 1.** Preparation and timeline of the experiments. (a) Schematic illustration of the basis of chemogenetic and optogenetic stimulations. AAVs were injected into the MRR (AP: −4.1 mm; L: 0 mm; DV: 4.6 mm from Bregma). In order to specifically target VGLUT3 + neurons, Cre-dependent AAVs (including lox2722 and loxP cleaving sites) encoded our target genes and a reporter protein in an opposite reading order, and VGLUT3-Cre mouse strains were used (males and females). In chemogenetics, we utilised DREADDs which were activated by intraperitoneal injection of CNO (1 mg/mL/kg), and expressed RFP as a reporter. With optogenetics, ChR2 was expressed, which is activated by blue laser (473 nm, 5 ms square pulse + 45 ms break, 20 Hz), and EYFP was used as a reporter. In both cases control animals received viral injections, but only the reporter protein was expressed. The brain slice shows a representation of a proper viral expression in a VGLUT3-Cre mouse, stained for anti-EYFP with Ni-DAB. (b) Timeline of the experiments. After the stereotaxic viral injections (indicated by schematic syringes and AAV vectors), incubation time for proper viral expression was at least 2 weeks. In the case of optogenetics, an additional 2-week recuperation and habituation was added after optic fiber implantation (indicated by schematic optic fiber). In order to ensure that the task for SRM is well learnt and the effect on spatial learning can be studied, the three days of cue task of the WM was executed (no CNO injection, or optogenetic excitation). Mobility and anxiety-like behaviour, major confounding factors for the outcome of WM, were measured by 10 min in the OF test and on the EPM. After 5 days of SRM task, a STM probe (at 10 mins) and a LTM probe (at 72 h) was conducted. Under the pictograms of OF, EPM and WM SRM task, the different excitation methods are represented. Chemogenetic excitation (CNO injection 30 mins before the start of OF, EPM and WM SRM task) is indicated by a pictogram showing a mouse being injected. Optogenetic excitation (at 20 Hz) during experiment (periphery in OF, center of EPM, 10 s while on the platform during WM SRM learning days) at 20 Hz. At the end of the experiments the animals were sacrificed and their brains were collected for viral expression validation. Abbreviations: AAVs: Adeno-associated viral vectors; AP: anterior-posterior; ChR2: Channelrhodopsin2; CNO: clozapine-N-oxide; DREADDs: designer receptors exclusively activated by designer drugs; DV: dorso-ventral; EPM: elevated plus maze; EYFP: enhanced yellow fluorescent protein; $G_q$: DREADD receptor inducing $G_q$ excitatory pathway; L: lateral; LTM: long-term memory probe; MRR: median raphe region; Ni-DAB: nickel-3.3′-diaminobenzidine; OF: open field; RFP: red fluorescent protein; SRM: spatial reference memory task; STM: short-term memory probe; VGLUT3: vesicular glutamate transporter type 3; WM: Watermaze test.

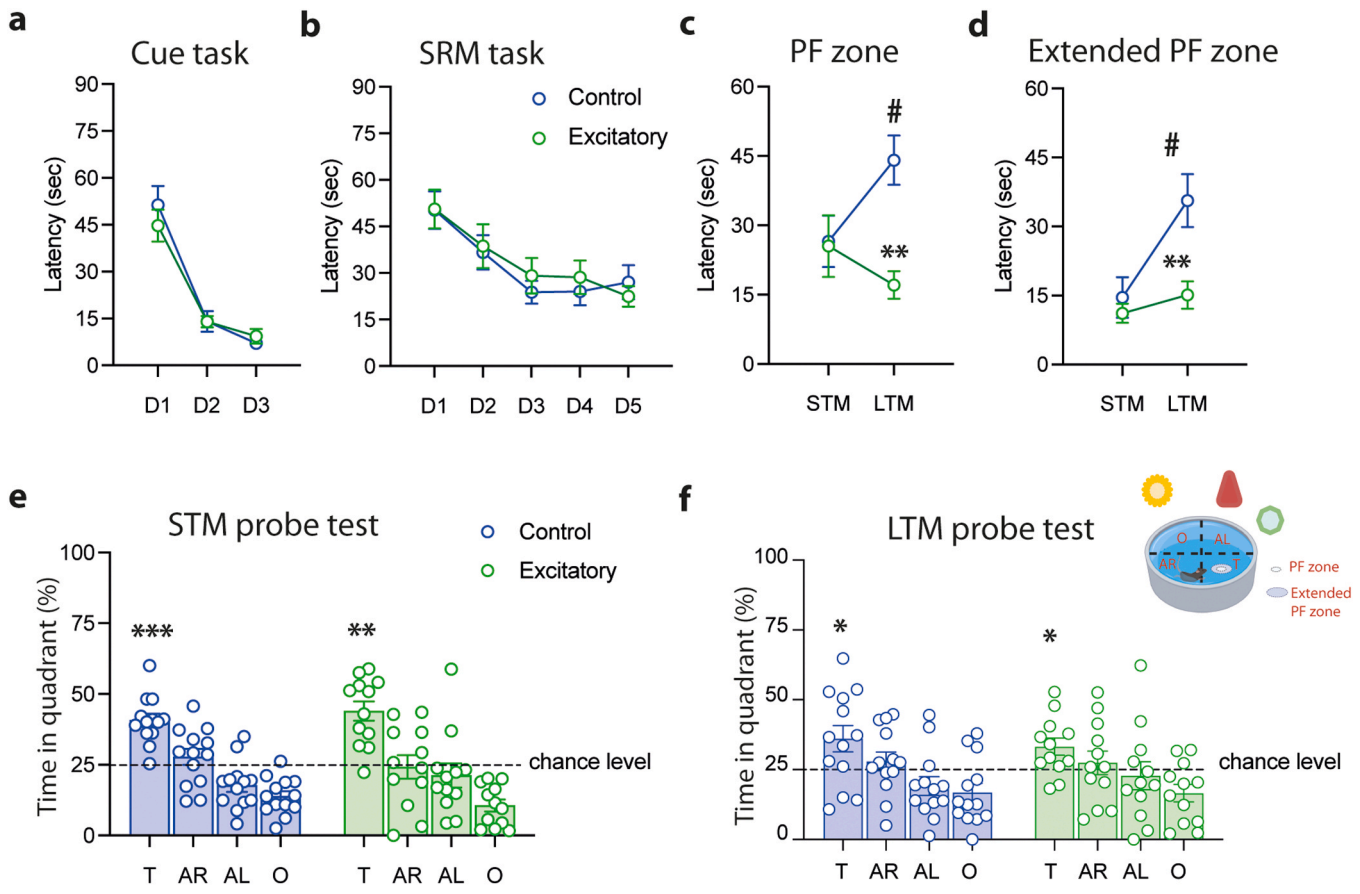


**Fig. 2. Results of chronic chemogenetic excitation of MRR-VGLUT3 + neurons. (a)** In the Cue task of the WM, all animals could learn the exercise, without differences between the groups (no manipulations). **(b)** Chemogenetic activation of the MRR VGLUT3 + neurons did not affect the learning curve during SRM task **(c)** With chemogenetics, there was long-term effect after the repeated excitation of the MRR VGLUT3 + neurons: animals found the (missing) platform and its approximate area (×2) **(d)** faster even 72 h later compared to the control mice, who showed natural decline in their performance. During STM, there was no difference between the groups. **(e)** Quadrant preference during STM probe (10 mins) exceeded the random chance (25%) for both the control and the excitatory groups. **(f)** During LTM probe, both group had higher than random chance (25%) preference for target quadrant. Insert: schematic representation of the WM paradigm. Mice had to learn the place of a platform (1 cm under the surface of the water) within time limit. Extramaze cues were provided. During STM and LTM probes, the platform was removed, and the latency to reach its exact placement (PF zone), or its approximate placement (×2 the original size; extended platform zone) within 60 s. Quadrants were labelled in relation to the target quadrant (that originally contained the platform): AR, AL and O. Data are expressed as mean±SEM. The detailed results and statistical tests of the replication cohort can be found on Supplementary Table 1. Abbreviations: AL: adjacent left; AR: adjacent right; CT: cue task; LTM: long-term memory; MRR: median raphe region; O: opposite; PF: platform; SRM: spatial reference memory; STM: short-term memory; T: target quadrant; VGLUT3: vesicular glutamate transporter type 3. **(c)** and **(d)**: # $p < 0.05$ vs STM probe; ** $p < 0.01$ vs control; **(e)** and **(f)**: *** $p < 0.0001$, ** $p < 0.0002$, * $p < 0.05$ vs random chance 25%.

recovery, mice were habituated to the patch cords by daily 10-minute training sessions to adapt to their weight and handling.

### 2.3. Behavioural testing

Watermaze (WM) experiments were conducted between 12 a.m. and 5 p.m., while open field (OF) and elevated plus-maze (EPM) tests took place between 9 a.m. and 2 p.m. The experiments were recorded by a ceiling-mounted camera (Samsung SNB 7000) and automatically analysed by ANY-maze (WM, France,) or Noldus Ethovision XT 15 (OF, EPM in France and Hungary, WM in Hungary). The experiments were performed as presented on the schematic timeline of Fig. 1**b.**

#### 2.3.1. Open field (OF) test

Animals were put into an empty white plastic arena (France: 50 × 50 × 40 cm, Hungary: 40 × 36 × 15 cm) for 10 min with a lightning of ~25 lux in the centre (75% of the floor surface). Distance moved, frequency and time spent in periphery and centre were analysed automatically.

#### 2.3.2. Elevated plus maze (EPM) test

Animals were placed onto the central zone of the EPM apparatus (67 × 7 × 30 cm, 50 cm above the floor). The mice could freely explore the apparatus for 5 min. The test was conducted with lightning of ~25 lux in the open arms.

The number of open arm entries, closed arm entries (anxiety-independent indicator of activity), total distance moved, and time spent in each compartment were measured automatically. Percentage of open arm entries, representing locomotor-independent anxiety (Pellow et al., 1985; Lister, 1987), were calculated based on the total amount of entries in open and closed arms as followed:

% of open arm entries = (number of open arm entries / sum of all arm entries) × 100

#### 2.3.3. Watermaze (WM) tasks

The WM study consisted of three phases: cue task (CT), spatial reference memory (SRM) task and the test phases (probes) (Daumas et al., 2017). The tanks (France: 1.6 m, Hungary: 1.8 m in diameter) were filled up with 21 ± 1°C water and made opaque with aquasol or white tempera (respectively in the two countries). The animals were

randomly divided into two equal batches, each of them having their separate random order of target quadrant and starting points. All mice were single caged 30 mins before the start of the experiment for chemogenetics studies, and at the time of the optic fibre implantation for the optogenetics study. Training consisted of 4 daily trials, each lasting a maximum of 90 s or until the animal found the platform (platform diameter: 9 cm in France, 10 cm in Hungary). Animals that failed to find the platform within the allotted time, were guided to it. Once on the platform, mice were allowed to rest for 10 s before removal and being placed under a heating lamp or on a heating pad.

Training started with the CT protocol which lasted 3 days with an intertrial interval (ITI) of 20 min. The tank was surrounded by curtains (~80 lux inside) to block external spatial cues. The platform, placed 1 cm below the water surface, was cued with a colourful 20 mL Falcon tube. Across trials, the platform was positioned to the centre of a different quadrant (northwest, southwest, northeast, southeast), and animals started from different points (north, south, west, east), always facing the wall. Learning was considered successful when animals could reach the cued platform within 15 s. No treatment was administrated during this phase.

The SRM task was used to assess spatial learning and memory. During this phase, the curtains were removed, and distal spatial cues in the room were continuously visible (~80 lux in the middle of the tank). For each cohort, one quadrant (northwest or southeast, hereafter referred to as the target quadrant) contained a hidden platform submerged 1 cm below the water surface. Training lasted 5 days with an ITI of 10 min.

Short-term (STM) and long-term memory (LTM) were assessed by running two 60 s probe trials in which the platform was removed. STM was tested 10 min after the final SRM training trial. To prevent memory extinction, an additional training trial was given immediately afterwards, but was not evaluated. LTM was assessed 72 h after the first probe trial.

#### 2.3.4. Chemogenetic excitation during experiments

Half an hour before of 1) the OF session, 2) the EPM session, and 3) the daily WM SRM training, animals received an intraperitoneal (ip.) injection of clozapine-N-oxide (CNO; Tocris Bioscience, CAT No.: 4936/10; 1 mg/10 mL/kg dissolved in dimethyl sulfoxide [DMSO; 0.25% of the final solution] and saline). Details of the replication chemogenetic experiment performed in Hungary are provided in the Supplementary Data, Supplementary Table 2 and 3.

#### 2.3.5. Optogenetic excitation during experiments

Before behavioural testing, fibre-optic patch cords (custom made, multimode optical fibre, 0.22 NA, low-OH Ø105 μm Core, FG105LCA, FT900KY tubing, End A: LC/PC, End B: LC/PC, and multimode optical fibre, 0.22 NA, low-OH Ø105 μm Core, FG105LCA, FT030 tubing, End 1: FC/APC, End:2 LC/PC, Thorlabs Corp.) were connected to the implanted ferrules. The patch cords collimated and guided the laser beams from the source (473 mm, low noise diode-pumped solid-state laser, Ikecool Corp.). Laser output was measured with a power meter (Coherent, Laser Check) and adjusted to $20 \pm 0.5$ mW net energy at continuous light emission. Stimulation was controlled automatically by Noldus Ethovision XT 15 and delivered at 20 Hz (5 ms square pulse + 45 ms break).

In the OF, the animals received stimulation whenever they entered and stayed in the periphery of the arena, to test whether activation elicited an anxiolytic effect as reported previously (Amilhon et al., 2010). Because of the test duration and the limitations of continuous optogenetic stimulation (e.g. tissue overheating, neuronal inhibition induced by overstimulation), stimulation was applied in altering 30 s ON and 30 s OFF periods whenever the animals were in the targeted compartment.

For the EPM task, stimulation was triggered when animals entered the central part of the maze, just before choosing between the open or closed arms.

During the WM SRM task, stimulation was applied during the 10 s period (only ON period) in which animals remained on the platform, whether they had found it by themselves or been guided to it. This time point was chosen based on previous studies suggesting a role of the MRR in consolidation (Sarihi et al., 1999; Wang et al., 2015a). No stimulation was delivered during the cue task, the STM or the LTM probes.

#### 2.3.6. Tissue collection

At the end of behavioural testing, animals were sacrificed and brains were collected for virus expression validation. For chemogenetic experiments, mice were euthanized (France: 0.5 mg/kg Euthasol; Ceva Santé Animale; for replication in Hungary, see Supplementary Data). Brains were fixed by transcardial perfusion with 4% paraformaldehyde (PFA) in phosphate-buffered saline (PBS) and post-fixed in PFA for 1 day. They were then transferred to PBS, sectioned at 30 μm thickness using a vibratome (Leica VT 1000S), and stored in 0.01% azide-PBS until further processing.

For optogenetic experiments, animals were decapitated, and their brains were fixed by immersion in 4% PFA for one day, then stored at 4°C in azide-PBS until further processing. Before sectioning, brains were incubated in10% glucose azide-PBS for at least 24 h. Sections (30 μm) were cut with a sliding microtome (Reichert) and stored in cryoprotectant at −20°C.

### 2.4. Immunohistochemistry and microscopy

Viral infection and expression were validated by immunohistochemistry using the same protocol in both laboratories. To verify the exact area of infection, nickel-3.3′-diaminobenzidine (Ni-DAB) staining was performed (detailed protocols in (Biro et al., 2017; Fazekas et al., 2021; Chaves et al., 2022)). Sections were incubated for 48 h at 4°C in primary antibody solution against RFP (rabbit anti-RFP, 1:4000, Rockland, #600–401–379) prepared in PBS containing 2% bovine serum albumin [BSA; Sigma-Aldrich] and 0.1% Triton X-100 [Sigma-Aldrich]. After rinsing, slices were incubated for 1 h in a biotinylated secondary antibody solution (donkey anti-rabbit solution,1:1000, Jackson, #711–065–152) diluted in PBS with 2% BSA. Signal amplification was performed using an avidin-biotin complex (ABC, 1:1000; Vector Laboratories). Immunoreactivity was visualized with DAB (10 mg/mL, Sigma-Aldrich) in presence of 1% $NiNH_4SO_4$ (Sigma-Aldrich) and 0.003% $H_2O_2$ (Sigma-Aldrich). Sections were mounted on slides using either TRIS (Sigma-Aldrich) or gelatin (G9391, Sigma-Aldrich), dehydrated through an ascending ethanol series or xylene, and cover slipped with Eukitt (Sigma-Aldrich) or Depex (Sigma-Aldrich).

Ni-DAB-stained sections were evaluated by light microscopy (France: Axioskop 2 plus, Zeiss; Hungary: Panoramic Midi II, 3DHistech). Viral expression was examined between −4.04 and −4.96 mm from Bregma (see Fig. 1a in (Fazekas et al., 2021) for an example of an accepted hit). Animals were excluded if staining was absent, unilateral, or extended into other brain regions (e.g., dorsal raphe). For chemogenetics, 25 out of 47 mice in the first cohort (France) and 27 out of 39 mice in the replication cohort (Hungary) met our strict inclusion criteria. For optogenetics, 25 out of 46 animals were included in the statistical analysis.

### 2.5. Statistical analysis

Statistical analyses were performed using GraphPad Prism version 8.0.0 for Windows, (GraphPad Software, San Diego, California USA, www.graphpad.com) and StatSoft10 (ANCOVA, StatSoft,Inc., Tulsa, OK).

Group differences (control vs. excitation) and sex effects (male vs. female) were analysed with two-way ANOVA for distance moved, frequency of arm entries and percentage of open arm entries. Time spent in different compartments (zone effect: periphery vs. centre in OF, closed arm vs. open arm in EPM) and latency to locate the platforms (probe

effect) were analysed with three-way repeated measures ANOVA (3way ANOVA). Time spent in the target quadrant during probe tests was compared to chance level (25%) using single-sample *t*-tests. For OF and EPM data, where the amount of optogenetic excitation was place-dependent and not fixed in duration, ANCOVA was used with the time (s) of laser activation (measured by Ethovision) as a covariate. Normality was assessed with the Shapiro-Wilks test, and homogeneity of variances with Spearman's test for heteroscedasticity. For repeated measures ANOVA, Geisser-Greenhouse corrections were applied when appropriate. Sidak's test was used for post hoc comparisons. Data are expressed as mean±SEM. Statistical significance was set at $p < 0.05$ with $0.05 < p < 0.1$ considered a marginal difference. Full details of the statistical results (effects, F-test/*t*-test results, degrees of freedom, p-values) are provided in the Supplementary Tables.

## 3. Results

### 3.1. Chronic chemogenetic excitation facilitates long-term memory formation

To rule out confounding factors, we first assessed the effects of MRR-VGLUT3 + stimulation on locomotor activity and anxiety-like behaviour. In both the EPM and OF tests, no statistically significant excitation effects were observed for the main parameters analysed (Table 1**,** Supplementary Table 1). Excitation only marginally decreased distance moved in the OF (2way ANOVA, excitation effect: $F_{(1,21)} = 3.387$, $p = 0.079$). Moreover, only control males displayed differential exploration times between centre and periphery, an effect absent in the excitatory group (3way ANOVA, zone effect: $F_{(1,21)} = 4.920$, $p = 0.038$; zone × sex interaction: $F_{(1,21)} = 6.106$, $p = 0.022$ - Sidak's multiple comparison: control males, periphery vs. centre $p = 0.018$; excitatory males, periphery vs centre $p = 0.986$). Importantly, there was no statistical difference between excitatory groups in the time spent in the centre, indicating no major effects of stimulation on locomotion and anxiety-like behaviour.

In the WM, animals were first trained in the Cue task (CT), without manipulation (that is, no CNO injection before trials). All mice successfully completed CT within 3 days (3way ANOVA, time effect: $F_{(1.335,28.04)} = 79.300$, $p < 0.001$ - Sidak's multiple comparison: $p < 0.05$ for all D1–3 comparisons), with no group or sex differences (Fig. 2**a,** Supplementary Table 1).

Subsequently, mice were trained in the SRM task. The injection of CNO happened from D1-D5, 30 min before the first trial. Both control and excitatory groups acquired the SRM task within 5 days (3way ANOVA, time effect: $F_{(3.594,75.48)} = 8.681$, $p < 0.001$ - Sidak's multiple comparison $0.001 < p < 0.1$ for D1 vs D2–5; Fig. 2**b,** Supplementary Table 1). Daily excitation of the MRR-VGLUT3 + neurons did not alter the learning curve, and by the final training day (D5), all animals reliably found the platform regardless of treatment.

STM was assess immediately after training. Both control and excitatory groups showed a significant preference for the target quadrant compared to chance level (25%) (single sample *t*-test: control group $t = 6.718$, df=12, $p < 0.0001$; excitatory group $t = 5.487$, df=11, $p < 0.0002$; Fig. 2**e,** Supplementary Table 1), with no difference between groups. Similarly, during LTM assessment, both grouped showed a significant preference for the target quadrant (single sample *t*-test: control group $t = 2.355$, df=12, $p = 0.036$; excitatory group $t = 2.704$, df=11, $p = 0.020$; Fig. 2**f,** Supplementary Table 1), again without a group effect. There were also no differences in the distance moved during either probe tests (Table 2, Supplementary Table 1). When latency to reach the platform location was analysed (Fig. 2**c,** Supplementary Table 1), female control mice displayed significantly higher latencies compared to all other groups (data not shown; 3way ANOVA, sex × excitation: $F_{(1,21)} = 8.908$, $p = 0.007$ – Sidak's multiple comparison $0.01 < p < 0.05$ female control vs all other groups). The 3way ANOVA also revealed a main effect of excitation ($F_{(1,21)} = 7.546$, $p = 0.012$), and a probe × excitation interaction ($F_{(1,21)} = 10.63$, $p = 0.004$). Post-hoc comparisons showed no group differences during STM probe ($p = 0.988$). However, while excitatory mice maintained low latencies across both STM and LTM probes ($p = 0.313$), control mice showed a significant increase in latency from STM to LTM ($p = 0.011$). Additionally, the values of the control group were significantly higher than the excitatory group during LTM probe ($p = 0.002$). This was confirmed by a significant difference in latency slopes between groups across probes (control=22.285±5.718; excitatory= −9.325±6.955, $t = 3.530$, df=23, $p = 0.002$). Latency to the extended (x2) platform zone showed a similar pattern (Fig. 2**d,** Supplementary Table 1). Control females again had the highest latencies (data not shown). While control mice displayed a natural extinction effect from STM to LTM probes ($p < 0.001$), excitatory mice showed no change between probes ($p = 0.657$). During the LTM probe, latencies were significantly higher in controls than in excitatory mice ($p = 0.002$). Swimming speed to the platform differed only during LTM (2way ANOVA, group effect: $F_{(1,21)} = 5.103$, $p = 0.035$; group × sex interaction: $F_{(1,21)} = 6.764$; $p = 0.017$). Post-hoc analysis indicated that female controls swam slower than the other three groups ($0.01 < p \leq 0.05$), but otherwise no differences were observed between excitatory and control groups (Table 2).

Together, these results suggest that chronic excitation of MRR-VGLUT3 + neurons facilitates long-term, but not short-term, memory performance, and may mitigate natural extinction processes.

**Table 1**
Effects of MRR-VGLUT3 + excitation on locomotion and anxiety-like behaviour in the chemogenetics experiments.

| Group | | Control | | Excitatory | |
|---|---|---|---|---|---|
| Sex | | female (n = 6) | male (n = 7) | female (n = 6) | male (n = 6) |
| OF | Total distance moved (cm) | 3983.145 ± 224.231 | 3861.139 ± 279.499 | 3308.678 ± 366.293 | 3460.167 ± 279.228 |
| | Time in centre (%) | 48.401 ± 2.420 | 34.173 ± 3.762 | 48.350 ± 4.572 | 43.585 ± 3.613 |
| EPM | Total distance moved (cm) | 2031.527 ± 203.351 | 2133.564 ± 215.358 | 1874.165 ± 242.029 | 2083.360 ± 206.010 |
| | Closed arms (frequency) | 26.500 ± 2.837 | 33.000 ± 4.152 | 26.667 ± 4.744 | 29.833 ± 3.478 |
| | Open arm entries (%) | 24.997 ±1.963 | 21.910 ± 4.961 | 28.396 ±1.565 | 26.766 ±4.597 |
| | Time in closed arms (%) | 80.179 ± 1.642 | 80.784 ± 3.041 | 81.885 ± 3.712 | 78.189 ± 3.056 |
| | Time in open arms (%) | 5.309 ± 1.341 | 6.699 ± 2.508 | 5.899 ± 2.100 | 9.123 ± 2.505 |

Excitation of the median raphe region (MRR) vesicular glutamate transporter 3 (VGLUT3) neurons did not affect behaviour in the open field (OF) or elevated plus maze (EPM) tests. Data are expressed as mean±SEM. See also Supplementary Table 1 for statistics.

### 3.2. Chemogenetic results are reproducible

The robustness and reproducibility of these findings were tested by repeating the experiments in a second laboratory using the commercial VGLUT3-Cre mouse strain (see Supplementary Data for details). As in the initial cohort, both CT and SRM learning phases were successfully completed without group differences (Supplementary Figure 1a **and b**). During probe tests, a significant probes × excitation interaction was observed for latency to the platform (3way ANOVA, $F_{(1,23)} = 12.160$, $p = 0.002$). Sidak's multiple comparison revealed that control mice showed an increase in latency between STM and LTM probes ($p = 0.027$), whereas excitatory mice showed only a marginal decrease

**Table 2**
Total distance moved and speed to reach platform on the probe days in Watermaze experiments.

| Group | | | Control | | Excitatory | |
|---|---|---|---|---|---|---|
| Sex | | | female (n = 6/n = 4) | male (n = 7/n = 8) | female (n = 6/n = 6) | male (n = 6/n = 7) |
| Chemogenetics | STM | Total distance moved (cm) | 1572.483 ± 95.7878 | 1751.200 ± 48.873 | 1698.267 ± 68.661 | 1640.333 ± 58.6078 |
| | | Speed to PF (cm/s) | 32.892 ± 2.773 | 46.240 ± 5.958 | 50.257 ± 8.347 | 42.478 ± 10.692 |
| | LTM | Total distance moved (cm) | 1680.883 ± 71.089 | 1836.743 ± 53.066 | 1803.233 ± 76.106 | 1720.117 ± 67.630 |
| | | Speed to PF (cm/s) | 28.015 ± 1.185 | 41.117 ± 4.136* | 42.967 ± 2.116* | 40.066 ± 3.377(*) |
| Optogenetics | STM | Total distance moved (cm) | 1386.7424 ± 148.723 | 1685.708 ± 68.791 | 1427.630 ± 118.664 | 1784.081 ± 89.918 |
| | | Speed (cm/s) | 23.573 ± 5.379 | 29.535 ± 5.825 | 23.517 ± 2.512 | 32.353 ± 3.359 |
| | LTM | Total distance moved (cm) | 1472.682 ± 129.560 | 1737.478 ± 69.822 | 1468.192 ± 101.818 | 1801.431 ± 77.014 |
| | | Speed (cm/s) | 21.955 ± 2.896 | 28.487 ± 1.426 | 23.247 ± 3.662 | 44.974 ± 14.402 |

During chemogenetic long-term memory [LTM] probes, both the excitation and the group × sex interaction were significant, whereas group differences were observed during short-term memory [STM]. In the optogenetic experiments, significant sex differences were found ($p < 0.01$ for both and long-term memory [LTM] probes), with females swimming less than males. Data are expressed as mean±SEM. Numbers in parentheses refer to sample sizes for chemogenetic (France) and optogenetic (Hungary) experiments, respectively. See also Supplementary Table 1**. and 3.** for statistics. (*) $p = 0.057$, *$p < 0.05$ vs control female.

($p = 0.092$). Latencies during the LTM probe were significantly different between groups ($p = 0.007$), a finding supported by slope analysis (control=18.663±5.308; excitatory= −15.215±8.832; $t = 3.34$, df=25 $p = 0.003$) (Supplementary Figure 1c). Latency to the extended (x2) platform zone showed only a marginal probe × excitation interaction (3way ANOVA, $F_{(1,23)} = 3.311$, $p = 0.082$), although the trend resembled that of the first experiment (Supplementary Figure 1d).

Together, the replication experiment produced results consistent with the original cohort, supporting the reliability and robustness of the observed behavioural effects. Detailed results and statistics for OF, EPM WM-CT and SRM tasks are provided in Supplementary Data**,** Supplementary Table 2 and 3**.**

### *3.3. Optogenetic excitation during acquisition does not affect memory performance*

Because chronic chemogenetic stimulation of MRR-VGLUT3 + neurons during the SRM training improved memory performance, we next asked whether restricting stimulation to the acquisition phase could account for this effect. To test this, we used an optogenetic approach (opto) to stimulate MRR-VGLUT3 + neurons specifically when animals reached the PF during training.

As in the chemogenetic study, we first assessed locomotor activity and anxiety-like behaviour (Table 3). In the OF, after adjusting for laser activity as covariate (2way ANCOVA, covariate: $F_{(1,19)} = 12.586$, $p = 0.002$), females moved significantly more than males (sex effect: $F_{(1,19)} = 14.563$, $p = 0.001$), with no excitation effect (Supplementary Table 4). For the anxiety-like behaviour, adjusting for laser activity as covariate revealed no significant main effects or interactions for time spent in centre. In the EPM, ontogenetic excitation of MRR-VGLUT3 cells in the central zone increased the time spent in the open arm (3way ANCOVA, $F_{(1,20)} = 4.796$, $p = 0.041$), but not the locomotion-independent parameter of open/total arm entries, where only a marginal sex effect was detected (3way ANCOVA, $F_{(1,20)} = 3.421$, $p = 0.079$), with higher values in females. Similarly, increased locomotion in the excitatory group was reflected by a frequency of closed arm entries (3way ANCOVA, $F_{(1,20)} = 8.898$, $p = 0.007$), but not by distance moved, where only marginal effects were observed (3way ANCOVA, $F_{(1,20)} = 3.278$, $p = 0.085$; Table 3**,** Supplementary Table 4). Thus, optogenetic excitation of MRR-VGLUT3 + neurons had only minor hyperlocomotory and anxiolytic effects.

**Table 3**
Mobility and anxiety-like behaviour in the optogenetics experiments.

| Group | | Control | | Excitatory | |
|---|---|---|---|---|---|
| Sex | | female (n = 4) | male (n = 8) | female (n = 6) | male (n = 7) |
| OF | Total distance moved (cm) | 5335.845 ± 768.531 | 3614.159 ± 136.816 | 8922.244 ± 980.814 | 4183.507 ± 530.292 |
| | Time in centre (%) | 40.163 ± 3.511 | 32.720 ± 3.622 | 24.385 ± 5.167 | 23.846 ± 2.884 |
| EPM | Total distance moved (cm) | 2388.182 ± 335.136 | 2296.032 ± 220.525 | 3166.213 ± 310.243 | 2792.891 ± 291.501 |
| | Closed arm (frequency) | 19.400 ± 1.691 | 26.286 ± 3.828 | 42.667 ± 6.711 | 35.714 ± 6.585 |
| | Open arm entries (%) | 24.556 ± 2.711 | 19.632 ± 3.610 | 28.479 ± 1.273 | 21.822 ± 1.453 |
| | Time in closed arms (%) | 85.096 ± 3.417 | 79.883 ± 4.116 | 61.716 ± 6.379 | 71.989 ± 4.281 |
| | Time in open arms (%) | 3.394 ± 1.405 | 5.062 ± 2.289 | 10.648 ± 2.017 | 7.634 ± 1.581 |

In the open field (OF), after adjusting for laser activity as covariate, females moved more than males, with no differences in anxiety-related parameters. In the elevated plus maze (EPM), excitation significantly affected closed arm entry frequency and the percentage of time spent in the open arms, indicating a modest anxiolytic effect. Data are expressed as mean±SEM. Statistical details are provided in Supplementary Table 4.

In the WM task, as in the chemogenetic experiments, all animals completed the CT (no manipulation) within 3 days (3way ANOVA, time effect: $F_{(1.508,30.16)} = 108.500$, $p < 0.001$; Sidak's multiple comparison: $p < 0.001$ for all D1 vs D2 vs D3; Fig. 3**a**). Female mice generally showed higher latencies than males (data not shown; 3way ANOVA, sex effect: $F_{(1,20)} = 5.638$, $p = 0.028$, Supplementary Table 4).

During the SRM task, females again displayed higher latencies (3way ANOVA, sex effect: $F_{(1,20)} = 10.860$, $p = 0.004$). A significant time × excitation interaction was also detected ($F_{(4,80)} = 3.794$, $p = 0.007$), although Sidak's multiple comparisons revealed no group or sex

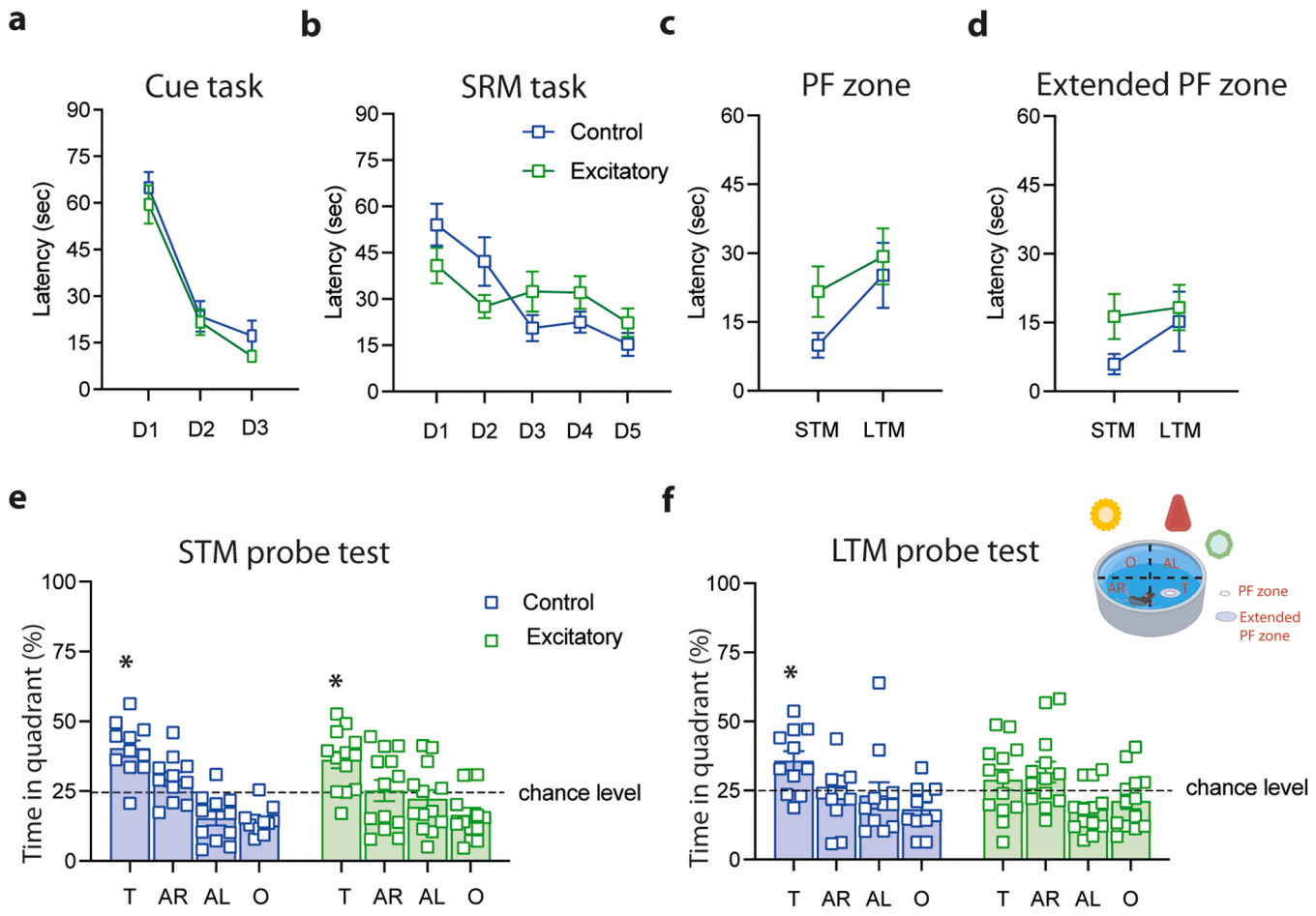


**Fig. 3. Results of acute optogenetic excitation of MRR-VGLUT3 + neurons. (a)** Similarly as before, all animals, without differences between the groups were able to learn the Cue task of WM (no manipulations). **(b)** Despite a significant interaction of time × excitation (3way ANOVA $F_{(4,80)}= 3.794$, $p = 0.007$), Sidak's multiple comparison did not reveal differences between the groups during SRM task for acute optogenetic activation of the MRR VGLUT3 + neurons. **(c)** Latency to find PF zone or its extended (×2) area **(d)** did not show differences between control and opto stimulated animals, just an overall increase between STM and LTM. **(e)** Quadrant preference during STM probe (10 mins) exceeded the random chance (25%) for both the control and the excitatory groups. **(f)** During LTM probe, only control animals had higher than random chance (25%) preference for target quadrant. Insert: schematic representation of the WM paradigm. Data are expressed as mean±SEM. The detailed statistical tests can be found in Supplementary Table 4. Abbreviations: AL: adjacent left; AR: adjacent right; CT: cue task; LTM: long-term memory; MRR: median raphe region; O: opposite; PF: platform; SRM: spatial reference memory; STM: short-term memory; T: target quadrant; VGLUT3: vesicular glutamate transporter type 3. * $p < 0.05$, vs random chance 25%.

differences (Fig. 3**b,** Supplementary Table 4). Learning was indicated by a general decrease in latency across training days (time effect: $F_{(3.126,62.52)}= 10.810$, $p < 0.001$).

In the STM probe, both groups showed significant preference for the target quadrant compared to chance (25%; single sample *t*-test: control, $t = 5.273$, df=10 $p < 0.001$; excitatory: $t = 3.786$, df=12, $p = 0.003$; Fig. 3**e**). In contrast, during LTM probe, only the control group showed significant preference (single sample *t*-test, $t = 3.101$, df=10, $p = 0.011$, Fig. 3**f**). However, no differences were observed between the groups in quadrant time or distance moved. Females generally exhibited lower values (2way ANOVA, sex effect: $F_{(1,20)}= 9.437$, $p = 0.006$, Table 2, Supplementary Table 4). Similarly, swimming speed to the platform place was lower in females (Table 2), though not significant. Latency analysis showed no differences between and excitatory groups. Both groups exhibited an overall increase in latency during LTM compared to STM, an effect absent when analysing the extended platform zone (Fig. 3**c,** Supplementary Table 4).

Thus, brief optogenetic excitation of MRR-VGLUT3 + neurons during PF acquisition did not facilitate memory, indicating that the behavioural effects observed with chemogenetics require prolonged stimulation and have a strict temporal prerequisite.

## 4. Discussion

Glutamatergic transmission plays a key role in learning and memory processes, but the specific role of VGLUT3 + projections from the MRR nucleus remains poorly understood. To address this, we used chemogenetic and optogenetic approaches to stimulate MRR-VGLUT3 + neurons during spatial reference memory acquisition and retrieval in the WM. While neither approach influenced spatial learning or STM (10 min), repeated chemogenetic stimulation improved LTM (72 h). This is consistent with the prolonged action of chemogenetics, as DREADD activation can be detected for hours after CNO administration (Alexander et al., 2009; Thompson et al., 2018), potentially covering both acquisition and consolidation phase. In contrast, optogenetic stimulation restricted to the platform acquisition phase was ineffective, highlighting a strict temporal dependency of MRR-VGLUT3 + involvement. Notably, with our chemogenetic protocol (i.e. STM ~1 h post CNO injection), possible confounding effects of direct stimulation during STM retrieval cannot be excluded. To check the robustness of our results, a replication cohort at a different laboratory was done, for which experimental conditions were matched as much as possible (i.e., same experimenter, timeline, AAVs, protocols, lighting conditions). The differences (e.g., ~10 s variation in latencies) are possibly due to the

separate colonies and strains established at the two locations. It has been shown in the literature that different strains (e.g., C57BL/6 N vs J) can show significantly different behavioural phenotypes (Simon et al., 2013; Ahlgren and Voikar, 2019), and we can see similar tendencies in our data. For example, in the OF, the replication cohort (C57BL6/J strain) had higher distance moved compared to the C57BL6/N mice in the chemogenetic experiments, or generally higher latencies in WM task, phenomenon also observed in literature (Simon et al., 2013; Ahlgren and Voikar, 2019). Unfortunately, due to high variability in the replication cohort, some parameters (e.g.: time spent in quadrant) did not match. Despite that, the latency to platform during WM probes showed the same statistical differences, strengthening our conclusions.

Regarding locomotor and anxiety-like behaviours, no consistent effects of MRR-VGLUT3 + excitation were detected. Studies in the literature examined the contribution of MRR or VGLUT3 + neurons to mobility and anxiety-like behaviour separately, indicating that both might affect these behaviours (Amilhon et al., 2010; Bland et al., 2016; Abela et al., 2020; Kljakic et al., 2022). Indeed, in our recently published work (Fazekas et al., 2024), we found that the chemogenetic inhibition of the MRR-VGLUT3 + neurons decreased the distance moved in open field, while excitation had no effect (only male, C57BL6/J mice), similarly to what we found in our current, separate study, confirming it both on females and another mouse strain (C57BL6/N). However, the previously observed anxiolytic effect of MRR-VGLUT3 + neuronal excitation on the EPM (Fazekas et al., 2024) was not replicated. Some studies have shown that anxiety-like behaviour might depend exhibited on the EPM might depend bot on the sex and circadian phase (light vs dark) (Verma et al., 2010; Nakano et al., 2016). Indeed, in our previous study (Fazekas et al., 2024) we conducted our experiment only in the dark phase, on male mice. It might be possible, that the anxiolytic effect of MRR-VGLUT3 + neuronal activity observed there was masked by the light phase and the mixture of female and male mice.

Sex differences were prominent, especially in the optogenetic experiments. Females ($24.500 \pm 0.629$ g) were lighter than males ($29.447 \pm 0.694$ g), which may explain higher locomotion in the OF but increased fatigue and platform latencies in the WM. Indeed, females generally show greater ambulation in OF tests (Tucker et al., 2016), although findings in WM are inconsistent: while a meta-analysis suggested female advantages (Jonasson, 2005), task conditions such as water vs. dry mazes yield opposite patterns. Interestingly, the first chemogenetic experimental group showed a strong difference in the swimming speed of female control animals (Table 2), which was not detected in any other experiment. This was probably an unspecific litter effect, as in this cohort all female controls showed it, regardless whether their viral expression was appropriate, off-target or non-detectable (data not shown). Literature indicates that there is no difference between the sexes regarding their performance in the WM task (Baldan Ramsey et al., 2010) , but might be a mouse strain effect (Ashworth et al., 2015) . As no other experiment, replication cohort, or alternative locomotion parameter showed such discrepancy, it is unlikely that our findings regarding memory are confounded by exploratory or anxiety factors.

Our study was motivated by the dense VGLUT3 + projections from the MRR to the hippocampus (Jackson et al., 2009; Szonyi et al., 2016; He et al., 2022; Fortin-Houde et al., 2023). MRR-VGLUT3 neurons represents around 26% of the MRR population (Sos et al., 2017) and form excitatory synapses in the hippocampus (Szonyi et al., 2016), where they influence oscillatory activity, thereby affecting memory consolidation (Ognjanovski et al., 2017; Xia et al., 2017). Non-serotonergic MRR activity decreases during hippocampal ripples, and stimulation supresses ripple events (Wang et al., 2015a). In contrast, long projecting GABAergic neurons positively correlate with theta and ripple oscillations, while VGLUT3 + neurons showed negative correlations, suggesting opposing roles for different MRR neuronal populations (Wang et al., 2015a; Jelitai et al., 2021). Moreover, GABAergic and VGLUT3 + , but not serotonergic, MRR neurons are phase-locked to theta activity (Huang et al., 2022), supporting the importance of investigating this subpopulation.

Recent work showed that chemogenetic inhibition (but not excitation) of MRR-VGLUT3 + neurons projecting to parvalbumin positive interneurons in the dentate gyrus impaired spatial memory acquisition without affecting locomotion or anxiety (He et al., 2022). Based on this, we expected enhanced learning with excitation. Instead, our results suggest a role in more downstream memory processes, reflected in preserved low PF latency during LTM probe in the excitatory MRR-VGLUT3-Cre mice. However, we must note that the projection described by He et al. (2022) is contradictory to multiple previous studies. According to those, in the hippocampus MRR afferents, especially that of VGLUT3 + , mainly innervate all other type of interneurons (e.g., 5-$HT_{3a}$R+/cholecystokinin positive, calbindin positive), but rarely (Aznar et al., 2004) or never parvalbumin positive ones (Freund et al., 1990; Halasy et al., 1992; Varga et al., 2009; Senft et al., 2021; Stinson and Ninan, 2024). Unfortunately, it was out of the scope of our study to address this contradiction. Nevertheless, it is well established, that MRR-VGLUT3 + neurons innervate and functionally regulate interneuronal activity in the hippocampus (Stinson and Ninan, 2024).

Hippocampal interneurons seem to have a role in the organisation of oscillations (Klausberger et al., 2003, 2005). Theta and ripple oscillations are central to memory consolidation (Kudrimoti et al., 1999; Buzsaki, 2015; Colgin, 2016), especially in spatial learning tasks (Ego-Stengel and Wilson, 2010; Aleman-Zapata et al., 2022). Hippocampal theta activity changes throughout the different phases of the Morris watermaze task (Olvera-Cortes et al., 2004; Hernandez-Perez et al., 2016). However, our temporally restricted optogenetic excitation did not alter learning or memory, suggesting that MRR-VGLUT3 + neurons may not directly regulate oscillations during acquisition. Instead, effects may emerge during sleep, when oscillations support consolidation (Buzsaki et al., 1983; Buzsaki, 1986; Louie and Wilson, 2001). During REM sleep, when theta oscillations are dominant in the hippocampus, MRR-VGLUT3 + neurons are silent, whereas their activity coincides with suppressed oscillations (Huang et al., 2022). Moreover, whole MRR stimulation after fear conditioning impaired consolidation (Wang et al., 2015a). Stinson and Ninan (2024) showed that MRR-VGLUT3 + neurons, that project onto 5-$HT_{3a}$R/cholecystokinin expressing neurons in the hippocampus, have an NMDA-mediated excitatory effect, and that indirectly causes the inhibition of CA1 pyramidal neurons. Interestingly, these 5-$HT_{3a}$R expressing interneurons seem to impair hippocampal gamma rhythm (Huang et al., 2016), an oscillation that has been implicated in the support of episodic memory encoding and retrieval (Griffiths and Jensen, 2023).

A limitation of our study is that we did not distinguish between purely VGLUT3 + and serotonin (5-HT)-VGLUT3 co-expressing neurons (Jackson et al., 2009; Senft et al., 2021). Up to 13% of the MRR-VGLUT3 + neurons co-express serotonin (Sos et al., 2017). These different MRR-VGLUT3 + subpopulations show distinct activity pattern and electrophysiological profiles, with VGLUT3 + /5-HT+ neurons displaying intermediate activity pattern between VGLUT3 + /5-HT- and VGLUT3-/5-HT+ neurons (Domonkos et al., 2016). How they affect spatial learning and memory formation is currently unknown, but such heterogeneity may contribute to contradictory findings on serotonergic involvement in hippocampus-dependent learning and memory processes (Coray and Quednow, 2022; Kazmierska-Grebowska et al., 2024). Indeed, inhibition of MRR serotonergic neurons (e.g.: via neurochemical lesion or 5-$HTR_{1A}$ activation) prevented the expression of contextual fear conditioning (Avanzi and Brandao, 2001; Avanzi et al., 2003; Almada et al., 2009). Additionally, prevention of serotoninergic transmission (e.g.: 5-$HTR_{1A}$ or 5-$HTR_7$ knockout, pharmacological blockade or optogenetic inhibition of terminals) in the dorsal hippocampus impaired spatial learning and memory (Sarnyai et al., 2000; Schmidt et al., 2017; Teixeira et al., 2018; Rodriguez et al., 2026). Recent evidence shows that MRR-VGLUT3 + neurons excite 5-$HTR_{3A}$ expressing GABAergic hippocampal neurons (Stinson and Ninan, 2024), highlighting complex glutamate-serotonin interactions. This further

demonstrates the need of cell-type specific investigations, and possibly in the future even the separate manipulations of VGLUT3 + /5-HT- and VGLUT3 + /5-HT+ neuronal populations.

It should be noted that our manipulation was not restricted to the MRR-hippocampus pathway (Fortin-Houde et al., 2023). The MRR-VGLUT3 + neurons also project to the prefrontal cortex and medial septum, both directly and through VGLUT3 + and/or GABAergic collaterals (Aznar et al., 2004; Jackson et al., 2009; Crooks et al., 2012; Szonyi et al., 2016). Both regions strongly influence hippocampal oscillations, and thus memory formation (Freund and Antal, 1988; Dragoi et al., 1999; Wang et al., 2015b; Jin et al., 2020; Gonzalez et al., 2022; Szabo et al., 2022). For example, in an Alzheimer's disease (AD) mouse model, Tau accumulation in the medial septum disrupts cholinergic hippocampal inputs and impairs spatial memory (Wu et al., 2021). Notably, lesions of the midbrain raphe nuclei has been reported in AD patients (Ebinger et al., 1987; Halliday et al., 1992). On the other hand, the MRR-VGLUT3 + cells projecting to the hippocampus also send collaterals to the medial prefrontal cortex (Szonyi et al., 2016), which may support prefrontal-hippocampal interactions critical for spatial decision-making (Tavares and Tort, 2022). Considering the anatomical connections of MRR and its VGLUT3 + neuronal population, it is a plausible theory that they modulate the activity of inhibitory neurons which shape hippocampal oscillations, thus, affecting memory related processes. Based on this, we hypothesise that in our case, behavioural effects likely reflected chemogenetic activation during rest phases, whereas optogenetic stimulation during task engagement was ineffective. This latter might also be due to inadequate choice of excitation frequency (20 Hz), that might not have been close enough to physiological firing pattern of MRR-VGLUT3 + neurons during this specific learning and memory task.

In conclusion, our findings demonstrate that chronic chemogenetic excitation of MRR-VGLUT3 + neurons enhanced long-term spatial reference memory precision in mice in a hippocampus-dependent task. Importantly, we replicated these effects in an independent laboratory using a different VGLUT3-Cre mouse strain, confirming their robustness. However, the effects were strictly time-dependent, since only the long lasting chemogenetic activation was effective, whereas temporally restricted optogenetic stimulation was not. Future studies should examine whether stimulation (both chemogenetic and optogenetic) during immobility or sleep can reproduce these chemogenetic effects, and disentangle the roles of VGLUT3 + /5-HT- and VGLUT3 + /5-HT+ subpopulations. Specifically identifying the populations that affect memory-promoting oscillations (gamma, theta, ripple, etc.) and investigating their projections in the hippocampus (and potentially in the prefrontal cortex and medial septum) will be a key step to understand how they shape behaviour. The discrepancies across studies and approaches underscore the complex, temporally precise, and cell-type-specific contribution of MRR circuits to hippocampus-dependent memory.

## CRediT authorship contribution statement

**Tiago Chaves:** Writing – review & editing, Methodology, Investigation. **Véronique Fabre:** Writing – review & editing, Supervision, Methodology. **Adrienn Szabó:** Writing – review & editing, Methodology, Investigation. **Pedro Correia:** Writing – review & editing, Methodology, Investigation. **Csilla Lea Fazekas:** Writing – original draft, Visualization, Resources, Project administration, Methodology, Investigation, Formal analysis, Data curation, Conceptualization. **Bibiána Török:** Writing – review & editing, Methodology, Investigation. **Dóra Zelena:** Writing – original draft, Supervision, Methodology, Investigation, Funding acquisition, Conceptualization. **Stéphanie Daumas:** Writing – original draft, Visualization, Supervision, Resources, Methodology, Funding acquisition, Formal analysis, Conceptualization.

## Funding sources

This study was supported by the National Research Development and Innovation Office of Hungary (grant numbers K141934, K138763); as well as by the Thematic Excellence Program 2021 Health Sub-program of the Ministry for Innovation and Technology in Hungary, within the framework of the TKP2021-EGA-16 project of the Pécs of University and by the Hungarian Brain Research Program 3.0 (NAP 3.0) 2022–2025. A bilateral Balaton Program supported the cooperative work (2021–1.2.4-TÉT-2021–00010; PHC 48077NJ). Lastly, we would like to thank Campus France and the French Government for supporting the mobility of young researchers via their joint-PhD program.

## Declaration of Competing Interest

The authors have nothing to declare.

None of the supporters had a further role in the study design; in the collection, analysis and interpretation of data; in the writing of the report; and in the decision to submit the paper for publication.

## Acknowledgements

We would like to thank the Behavioral Studies Unit at the Institute of Experimental Medicine in Hungary and the CEFI and Behavioral Core Facility at Sorbonne Université, France for animals care and for providing appropriate environments for conducting behavioural experiments. The authors also wish to thank the Nikon Centre of Excellence at the Institute of Experimental Medicine, Nikon Austria GmbH and Auro-Science Consulting Ltd for kindly providing microscopy support. Lastly, we would like to thank Campus France and the French Government for supporting the mobility of young researchers via their joint-PhD program.

## Appendix A. Supporting information

Supplementary data associated with this article can be found in the online version at doi:10.1016/j.pneurobio.2026.102904.

## Data Availability

The datasets generated and/or analysed during the current study are available from the corresponding author on reasonable request.

## References

Abela, A.R., Browne, C.J., Sargin, D., Prevot, T.D., Ji, X.D., Li, Z., Lambe, E.K., Fletcher, P.J., 2020. Median raphe serotonin neurons promote anxiety-like behavior via inputs to the dorsal hippocampus. Neuropharmacology 168, 107985.

Ahlgren, J., Voikar, V., 2019. Experiments done in Black-6 mice: what does it mean? Lab Anim. (NY) 48, 171–180.

Aleman-Zapata, A., Morris, R.G.M., Genzel, L., 2022. Sleep deprivation and hippocampal ripple disruption after one-session learning eliminate memory expression the next day. Proc. Natl. Acad. Sci. USA 119, e2123424119.

Alexander, G.M., Rogan, S.C., Abbas, A.I., Armbruster, B.N., Pei, Y., Allen, J.A., Nonneman, R.J., Hartmann, J., Moy, S.S., Nicolelis, M.A., McNamara, J.O., Roth, B. L., 2009. Remote control of neuronal activity in transgenic mice expressing evolved G protein-coupled receptors. Neuron 63, 27–39.

Almada, R.C., Borelli, K.G., Albrechet-Souza, L., Brandao, M.L., 2009. Serotonergic mechanisms of the median raphe nucleus-dorsal hippocampus in conditioned fear: output circuit involves the prefrontal cortex and amygdala. Behav. Brain Res 203, 279–287.

Amilhon, B., Lepicard, E., Renoir, T., Mongeau, R., Popa, D., Poirel, O., Miot, S., Gras, C., Gardier, A.M., Gallego, J., Hamon, M., Lanfumey, L., Gasnier, B., Giros, B., El Mestikawy, S., 2010. VGLUT3 (vesicular glutamate transporter type 3) contribution to the regulation of serotonergic transmission and anxiety. J. Neurosci. 30, 2198–2210.

Ashworth, A., Bardgett, M.E., Fowler, J., Garber, H., Griffith, M., Curran, C.P., 2015. Comparison of Neurological Function in Males and Females from Two Substrains of C57BL/6 Mice. Toxics 3, 1–17.

Avanzi, V., Brandao, M.L., 2001. Activation of somatodendritic 5-HT(1A) autoreceptors in the median raphe nucleus disrupts the contextual conditioning in rats. Behav. Brain Res 126, 175–184.

Avanzi, V., Silva, R.C., Macedo, C.E., Brandao, M.L., 2003. 5-HT mechanisms of median raphe nucleus in the conditioned freezing caused by light/foot-shock association. Physiol. Behav. 78, 471–477.
Aznar, S., Qian, Z.X., Knudsen, G.M., 2004. Non-serotonergic dorsal and median raphe projection onto parvalbumin- and calbindin-containing neurons in hippocampus and septum. Neuroscience 124, 573–581.
Balazsfi, D., Zelena, D., Demeter, K., Miskolczi, C., Varga, Z.K., Nagyvaradi, A., Nyiri, G., Cserep, C., Baranyi, M., Sperlagh, B., Haller, J., 2018. Differential Roles of the Two Raphe Nuclei in Amiable Social Behavior and Aggression - An Optogenetic Study. Front Behav. Neurosci. 12, 163.
Balazsfi, D.G., Zelena, D., Farkas, L., Demeter, K., Barna, I., Cserep, C., Takacs, V.T., Nyiri, G., Goloncser, F., Sperlagh, B., Freund, T.F., Haller, J., 2017. Median raphe region stimulation alone generates remote, but not recent fear memory traces. PLoS One 12, e0181264.
Baldan Ramsey, L.C., Pittenger, C., 2010. Cued and spatial learning in the water maze: equivalent learning in male and female mice. Neurosci Lett 483, 148–151.
Biro, L., Toth, M., Sipos, E., Bruzsik, B., Tulogdi, A., Bendahan, S., Sandi, C., Haller, J., 2017. Structural and functional alterations in the prefrontal cortex after post-weaning social isolation: relationship with species-typical and deviant aggression. Brain Struct. Funct. 222, 1861–1875.
Bland, B.H., Bland, C.E., MacIver, M.B., 2016. Median raphe stimulation-induced motor inhibition concurrent with suppression of type 1 and type 2 hippocampal theta. Hippocampus 26, 289–300.
Buzsaki, G., 1986. Hippocampal sharp waves: their origin and significance. Brain Res 398, 242–252.
Buzsaki, G., 2015. Hippocampal sharp wave-ripple: A cognitive biomarker for episodic memory and planning. Hippocampus 25, 1073–1188.
Buzsaki, G., Leung, L.W., Vanderwolf, C.H., 1983. Cellular bases of hippocampal EEG in the behaving rat. Brain Res 287, 139–171.
Chaves, T., Torok, B., Fazekas, C.L., Correia, P., Sipos, E., Varkonyi, D., Hellinger, A., Erk, D., Zelena, D., 2022. Median raphe region GABAergic neurons contribute to social interest in mouse. Life Sci. 289, 120223.
Colgin, L.L., 2016. Rhythms of the hippocampal network. Nat. Rev. Neurosci. 17, 239–249.
Coray, R., Quednow, B.B., 2022. The role of serotonin in declarative memory: A systematic review of animal and human research. Neurosci. Biobehav Rev. 139, 104729.
Crooks, R., Jackson, J., Bland, B.H., 2012. Dissociable pathways facilitate theta and non-theta states in the median raphe–septohippocampal circuit. Hippocampus 22, 1567–1576.
Danieli, K., Guyon, A., Bethus, I., 2023. Episodic Memory formation: a review of complex Hippocampus input pathways. Prog. Neuropsychopharmacol. Biol. Psychiatry 126, 110757.
Daumas, S., Hunter, C.J., Mistry, R.B., More, L., Privitera, L., Cooper, D.D., Reyskens, K. M., Flynn, H.T., Morris, R.G., Arthur, J.S., Frenguelli, B.G., 2017. The Kinase Function of MSK1 Regulates BDNF Signaling to CREB and Basal Synaptic Transmission, But Is Not Required for Hippocampal Long-Term Potentiation or Spatial Memory. eNeuro 4.
Domonkos, A., Nikitidou Ledri, L., Laszlovszky, T., Cserep, C., Borhegyi, Z., Papp, E., Nyiri, G., Freund, T.F., Varga, V., 2016. Divergent in vivo activity of non-serotonergic and serotonergic VGluT3-neurones in the median raphe region. J. Physiol. 594, 3775–3790.
Dragoi, G., Carpi, D., Recce, M., Csicsvari, J., Buzsaki, G., 1999. Interactions between hippocampus and medial septum during sharp waves and theta oscillation in the behaving rat. J. Neurosci. 19, 6191–6199.
Ebinger, G., Bruyland, M., Martin, J.J., Herregodts, P., Cras, P., Michotte, Y., Gomme, L., 1987. Distribution of biogenic amines and their catabolites in brains from patients with Alzheimer's disease. J. Neurol. Sci. 77, 267–283.
Ego-Stengel, V., Wilson, M.A., 2010. Disruption of ripple-associated hippocampal activity during rest impairs spatial learning in the rat. Hippocampus 20, 1–10.
Eremin, D.V., Kondaurova, E.M., Rodnyy, A.Y., Molobekova, C.A., Kudlay, D.A., Naumenko, V.S., 2023. Serotonin Receptors as a Potential Target in the Treatment of Alzheimer's Disease. Biochemistry (Mosc 88, 2023–2042.
Fazekas, C.L., Bellardie, M., Torok, B., Sipos, E., Toth, B., Baranyi, M., Sperlagh, B., Dobos-Kovacs, M., Chaillou, E., Zelena, D., 2021. Pharmacogenetic excitation of the median raphe region affects social and depressive-like behavior and core body temperature in male mice. Life Sci. 286, 120037.
Fazekas, C.L., Torok, B., Correia, P., Chaves, T., Bellardie, M., Sipos, E., Horvath, H.R., Gaszner, B., Dora, F., Dobolyi, A., Zelena, D., 2024. The Role of Vesicular Glutamate Transporter Type 3 in Social Behavior, with a Focus on the Median Raphe Region. eNeuro 11.
Fortin-Houde, J., Henderson, F., Dumas, S., Ducharme, G., Amilhon, B., 2023. Parallel streams of raphe VGLUT3-positive inputs target the dorsal and ventral hippocampus in each hemisphere. J. Comp. Neurol. 531, 702–719.
Fremeau Jr., R.T., Burman, J., Qureshi, T., Tran, C.H., Proctor, J., Johnson, J., Zhang, H., Sulzer, D., Copenhagen, D.R., Storm-Mathisen, J., Reimer, R.J., Chaudhry, F.A., Edwards, R.H., 2002. The identification of vesicular glutamate transporter 3 suggests novel modes of signaling by glutamate. Proc. Natl. Acad. Sci. USA 99, 14488–14493.
Freund, T.F., 1992. GABAergic septal and serotonergic median raphe afferents preferentially innervate inhibitory interneurons in the hippocampus and dentate gyrus. Epilepsy Res Suppl. 7, 79–91.
Freund, T.F., Antal, M., 1988. GABA-containing neurons in the septum control inhibitory interneurons in the hippocampus. Nature 336, 170–173.
Freund, T.F., Gulyas, A.I., Acsady, L., Gorcs, T., Toth, K., 1990. Serotonergic control of the hippocampus via local inhibitory interneurons. Proc. Natl. Acad. Sci. USA 87, 8501–8505.
Geldenhuys, W.J., Van der Schyf, C.J., 2011. Role of serotonin in Alzheimer's disease: a new therapeutic target? CNS Drugs 25, 765–781.
Gonzalez, M.C., Radiske, A., Rossato, J.I., Conde-Ocazionez, S., Bevilaqua, L.R.M., Cammarota, M., 2022. Optogenetic inactivation of the medial septum impairs long-term object recognition memory formation. Mol. Brain 15, 50.
Gras, C., Herzog, E., Bellenchi, G.C., Bernard, V., Ravassard, P., Pohl, M., Gasnier, B., Giros, B., El Mestikawy, S., 2002. A third vesicular glutamate transporter expressed by cholinergic and serotoninergic neurons. J. Neurosci. 22, 5442–5451.
Gras, C., Amilhon, B., Lepicard, E.M., Poirel, O., Vinatier, J., Herbin, M., Dumas, S., Tzavara, E.T., Wade, M.R., Nomikos, G.G., Hanoun, N., Saurini, F., Kemel, M.L., Gasnier, B., Giros, B., El Mestikawy, S., 2008. The vesicular glutamate transporter VGLUT3 synergizes striatal acetylcholine tone. Nat. Neurosci. 11, 292–300.
Griffiths, B.J., Jensen, O., 2023. Gamma oscillations and episodic memory. Trends Neurosci. 46, 832–846.
Halasy, K., Miettinen, R., Szabat, E., Freund, T.F., 1992. GABAergic Interneurons are the Major Postsynaptic Targets of Median Raphe Afferents in the Rat Dentate Gyrus. Eur. J. Neurosci. 4, 144–153.
Halliday, G.M., McCann, H.L., Pamphlett, R., Brooks, W.S., Creasey, H., McCusker, E., Cotton, R.G., Broe, G.A., Harper, C.G., 1992. Brain stem serotonin-synthesizing neurons in Alzheimer's disease: a clinicopathological correlation. Acta Neuropathol. 84, 638–650.
He, A., Zhang, C., Ke, X., Yi, Y., Yu, Q., Zhang, T., Yu, H., Du, H., Li, H., Tian, Q., Zhu, L. Q., Lu, Y., 2022. VGLUT3 neurons in median raphe control the efficacy of spatial memory retrieval via ETV4 regulation of VGLUT3 transcription. Sci. China Life Sci. 65, 1590–1607.
Hernandez-Perez, J.J., Gutierrez-Guzman, B.E., Olvera-Cortes, M.E., 2016. Hippocampal strata theta oscillations change their frequency and coupling during spatial learning. Neuroscience 337, 224–241.
Huang, W., Ikemoto, S., Wang, D.V., 2022. Median Raphe Nonserotonergic Neurons Modulate Hippocampal Theta Oscillations. J. Neurosci. 42, 1987–1998.
Huang, Y., Yoon, K., Ko, H., Jiao, S., Ito, W., Wu, J.Y., Yung, W.H., Lu, B., Morozov, A., 2016. 5-HT3a Receptors Modulate Hippocampal Gamma Oscillations by Regulating Synchrony of Parvalbumin-Positive Interneurons. Cereb. Cortex 26, 576–585.
Jackson, J., Dickson, C.T., Bland, B.H., 2008. Median raphe stimulation disrupts hippocampal theta via rapid inhibition and state-dependent phase reset of theta-related neural circuitry. J. Neurophysiol. 99, 3009–3026.
Jackson, J., Bland, B.H., Antle, M.C., 2009. Nonserotonergic projection neurons in the midbrain raphe nuclei contain the vesicular glutamate transporter VGLUT3. Synapse 63, 31–41.
Jelitai, M., Barth, A.M., Komlosi, F., Freund, T.F., Varga, V., 2021. Activity and Coupling to Hippocampal Oscillations of Median Raphe GABAergic Cells in Awake Mice. Front Neural Circuits 15, 784034.
Jin, T., Chen, R., Shao, M., Yang, X., Ma, L., Wang, F., 2020. Dorsal hippocampus- and ACC-projecting medial septum neurons differentially contribute to the recollection of episodic-like memory. FASEB J. 34, 11741–11753.
Jonasson, Z., 2005. Meta-analysis of sex differences in rodent models of learning and memory: a review of behavioral and biological data. Neurosci Biobehav Rev 28, 811–825.
Kazmierska-Grebowska, P., Zakowski, W., Myslinska, D., Sahu, R., Jankowski, M.M., 2024. Revisiting serotonin's role in spatial memory: A call for sensitive analytical approaches. Int J. Biochem Cell Biol. 176, 106663.
Klausberger, T., Magill, P.J., Marton, L.F., Roberts, J.D., Cobden, P.M., Buzsaki, G., Somogyi, P., 2003. Brain-state- and cell-type-specific firing of hippocampal interneurons in vivo. Nature 421, 844–848.
Klausberger, T., Marton, L.F., O'Neill, J., Huck, J.H., Dalezios, Y., Fuentealba, P., Suen, W.Y., Papp, E., Kaneko, T., Watanabe, M., Csicsvari, J., Somogyi, P., 2005. Complementary roles of cholecystokinin- and parvalbumin-expressing GABAergic neurons in hippocampal network oscillations. J. Neurosci. 25, 9782–9793.
Kljakic, O., Hogan-Cann, A.E., Yang, H., Dover, B., Al-Onaizi, M., Prado, M.A.M., Prado, V.F., 2022. Chemogenetic activation of VGLUT3-expressing neurons decreases movement. Eur. J. Pharm. 935, 175298.
Kohler, C., Steinbusch, H., 1982. Identification of serotonin and non-serotonin-containing neurons of the mid-brain raphe projecting to the entorhinal area and the hippocampal formation. A combined immunohistochemical and fluorescent retrograde tracing study in the rat brain. Neuroscience 7, 951–975.
Kudrimoti, H.S., Barnes, C.A., McNaughton, B.L., 1999. Reactivation of hippocampal cell assemblies: effects of behavioral state, experience, and EEG dynamics. J. Neurosci. 19, 4090–4101.
Lister, R.G., 1987. The use of a plus-maze to measure anxiety in the mouse. Psychopharmacol. (Berl. ) 92, 180–185.
Louie, K., Wilson, M.A., 2001. Temporally structured replay of awake hippocampal ensemble activity during rapid eye movement sleep. Neuron 29, 145–156.
Maru, E., Takahashi, L.K., Iwahara, S., 1979. Effects of median raphe nucleus lesions on hippocampal EEG in the freely moving rat. Brain Res 163, 223–234.
Matsuo, N., Takao, K., Nakanishi, K., Yamasaki, N., Tanda, K., Miyakawa, T., 2010. Behavioral profiles of three C57BL/6 substrains. Front Behav. Neurosci. 4, 29.
McKenna, J.T., Vertes, R.P., 2001. Collateral projections from the median raphe nucleus to the medial septum and hippocampus. Brain Res Bull. 54, 619–630.
Melik, E., Babar-Melik, E., Ozgunen, T., Binokay, S., 2000. Median raphe nucleus mediates forming long-term but not short-term contextual fear conditioning in rats. Behav. Brain Res 112, 145–150.
Montkowski, A., Poettig, M., Mederer, A., Holsboer, F., 1997. Behavioural performance in three substrains of mouse strain 129. Brain Res 762, 12–18.
Munafo, M.R., Nosek, B.A., Bishop, D.V.M., Button, K.S., Chambers, C.D., du Sert, N.P., Simonsohn, U., Wagenmakers, E.J., Ware, J.J., Ioannidis, J.P.A., 2017. A manifesto for reproducible science. Nat. Hum. Behav. 1, 0021.

Nakano, J.J., Shimizu, K., Shimba, S., Fukada, Y., 2016. SCOP/PHLPP1beta in the basolateral amygdala regulates circadian expression of mouse anxiety-like behavior. Sci. Rep. 6, 33500.
Ognjanovski, N., Schaeffer, S., Wu, J., Mofakham, S., Maruyama, D., Zochowski, M., Aton, S.J., 2017. Parvalbumin-expressing interneurons coordinate hippocampal network dynamics required for memory consolidation. Nat. Commun. 8, 15039.
Olvera-Cortes, E., Guevara, M.A., Gonzalez-Burgos, I., 2004. Increase of the hippocampal theta activity in the Morris water maze reflects learning rather than motor activity. Brain Res Bull. 62, 379–384.
Pellow, S., Chopin, P., File, S.E., Briley, M., 1985. Validation of open:closed arm entries in an elevated plus-maze as a measure of anxiety in the rat. J. Neurosci. Methods 14, 149–167.
Rodriguez, G., Zhao, X., Neugebauer, N.M., Meltzer, H.Y., Dong, H., 2026. Impact of 5-HT7 receptor gene deletion on memory and affective behaviors in young and aged mice. Neuroscience 592, 191–200.
Sarihi, A., Motamedi, F., Rashidy-Pour, A., Naghdi, N., Behzadi, G., 1999. Reversible inactivation of the median raphe nucleus enhances consolidation and retrieval but not acquisition of passive avoidance learning in rats. Brain Res 817, 59–66.
Sarnyai, Z., Sibille, E.L., Pavlides, C., Fenster, R.J., McEwen, B.S., Toth, M., 2000. Impaired hippocampal-dependent learning and functional abnormalities in the hippocampus in mice lacking serotonin(1A) receptors. Proc. Natl. Acad. Sci. USA 97, 14731–14736.
Schafer, M.K., Varoqui, H., Defamie, N., Weihe, E., Erickson, J.D., 2002. Molecular cloning and functional identification of mouse vesicular glutamate transporter 3 and its expression in subsets of novel excitatory neurons. J. Biol. Chem. 277, 50734–50748.
Schmidt, S.D., Furini, C.R.G., Zinn, C.G., Cavalcante, L.E., Ferreira, F.F., Behling, J.A.K., Myskiw, J.C., Izquierdo, I., 2017. Modulation of the consolidation and reconsolidation of fear memory by three different serotonin receptors in hippocampus. Neurobiol. Learn Mem. 142, 48–54.
Senft, R.A., Freret, M.E., Sturrock, N., Dymecki, S.M., 2021. Neurochemically and Hodologically Distinct Ascending VGLUT3 versus Serotonin Subsystems Comprise the r2-Pet1 Median Raphe. J. Neurosci. 41, 2581–2600.
Silva, R.C., Cruz, A.P., Avanzi, V., Landeira-Fernandez, J., Brandao, M.L., 2002. Distinct contributions of median raphe nucleus to contextual fear conditioning and fear-potentiated startle. Neural Plast. 9, 233–247.
Simon, M.M., et al., 2013. A comparative phenotypic and genomic analysis of C57BL/6J and C57BL/6N mouse strains. Genome Biol. 14, R82.
Sos, K.E., Mayer, M.I., Cserep, C., Takacs, F.S., Szonyi, A., Freund, T.F., Nyiri, G., 2017. Cellular architecture and transmitter phenotypes of neurons of the mouse median raphe region. Brain Struct. Funct. 222, 287–299.
Stinson, H.E., Ninan, I., 2024. Median raphe glutamatergic neuron-mediated enhancement of GABAergic transmission and suppression of long-term potentiation in the hippocampus. Heliyon 10, e38192.
Sultana, R., Ogundele, O.M., Lee, C.C., 2019. Contrasting characteristic behaviours among common laboratory mouse strains. R. Soc. Open Sci. 6, 190574.
Szabo, G.G., Farrell, J.S., Dudok, B., Hou, W.H., Ortiz, A.L., Varga, C., Moolchand, P., Gulsever, C.I., Gschwind, T., Dimidschstein, J., Capogna, M., Soltesz, I., 2022. Ripple-selective GABAergic projection cells in the hippocampus. Neuron 110, 1959–1977 e1959.
Szonyi, A., Mayer, M.I., Cserep, C., Takacs, V.T., Watanabe, M., Freund, T.F., Nyiri, G., 2016. The ascending median raphe projections are mainly glutamatergic in the mouse forebrain. Brain Struct. Funct. 221, 735–751.
Szonyi, A., Zicho, K., Barth, A.M., Gonczi, R.T., Schlingloff, D., Torok, B., Sipos, E., Major, A., Bardoczi, Z., Sos, K.E., Gulyas, A.I., Varga, V., Zelena, D., Freund, T.F., Nyiri, G., 2019. Median raphe controls acquisition of negative experience in the mouse. Science 366.
Tavares, L.C.S., Tort, A.B.L., 2022. Hippocampal-prefrontal interactions during spatial decision-making. Hippocampus 32, 38–54.
Teixeira, C.M., Rosen, Z.B., Suri, D., Sun, Q., Hersh, M., Sargin, D., Dincheva, I., Morgan, A.A., Spivack, S., Krok, A.C., Hirschfeld-Stoler, T., Lambe, E.K., Siegelbaum, S.A., Ansorge, M.S., 2018. Hippocampal 5-HT input regulates memory formation and schaffer collateral excitation. Neuron 98, 992–1004 e1004.
Thompson, K.J., et al., 2018. DREADD Agonist 21 Is an effective agonist for muscarinic-based DREADDs in Vitro and in Vivo. ACS Pharm. Transl. Sci. 1, 61–72.
Tucker, L.B., Fu, A.H., McCabe, J.T., 2016. Performance of Male and Female C57BL/6J mice on motor and cognitive tasks commonly used in pre-clinical traumatic brain injury research. J. Neurotrauma 33, 880–894.
Van Dam, D., Lenders, G., De Deyn, P.P., 2006. Effect of Morris water maze diameter on visual-spatial learning in different mouse strains. Neurobiol. Learn Mem. 85, 164–172.
Vann, S.D., Albasser, M.M., 2011. Hippocampus and neocortex: recognition and spatial memory. Curr. Opin. Neurobiol. 21, 440–445.
Varga, V., Losonczy, A., Zemelman, B.V., Borhegyi, Z., Nyiri, G., Domonkos, A., Hangya, B., Holderith, N., Magee, J.C., Freund, T.F., 2009. Fast synaptic subcortical control of hippocampal circuits. Science 326, 449–453.
Verma, P., Hellemans, K.G., Choi, F.Y., Yu, W., Weinberg, J., 2010. Circadian phase and sex effects on depressive/anxiety-like behaviors and HPA axis responses to acute stress. Physiol. Behav. 99, 276–285.
Viana Di Prisco, G., Albo, Z., Vertes, R.P., Kocsis, B., 2002. Discharge properties of neurons of the median raphe nucleus during hippocampal theta rhythm in the rat. Exp. Brain Res 145, 383–394.
Wang, D.V., Yau, H.J., Broker, C.J., Tsou, J.H., Bonci, A., Ikemoto, S., 2015a. Mesopontine median raphe regulates hippocampal ripple oscillation and memory consolidation. Nat. Neurosci. 18, 728–735.
Wang, Y., Romani, S., Lustig, B., Leonardo, A., Pastalkova, E., 2015b. Theta sequences are essential for internally generated hippocampal firing fields. Nat. Neurosci. 18, 282–288.
Wu, D., Gao, D., Yu, H., Pi, G., Xiong, R., Lei, H., Wang, X., Liu, E., Ye, J., Yu, H., Gao, Y., He, T., Jiang, T., Sun, F., Su, J., Song, G., Peng, W., Yang, Y., Wang, J.Z., 2021. Medial septum tau accumulation induces spatial memory deficit via disrupting medial septum-hippocampus cholinergic pathway. Clin. Transl. Med 11, e428.
Xia, F., Richards, B.A., Tran, M.M., Josselyn, S.A., Takehara-Nishiuchi, K., Frankland, P. W., 2017. Parvalbumin-positive interneurons mediate neocortical-hippocampal interactions that are necessary for memory consolidation. Elife 6.
Zander, J.F., Munster-Wandowski, A., Brunk, I., Pahner, I., Gomez-Lira, G., Heinemann, U., Gutierrez, R., Laube, G., Ahnert-Hilger, G., 2010. Synaptic and vesicular coexistence of VGLUT and VGAT in selected excitatory and inhibitory synapses. J. Neurosci. 30, 7634–7645.